JOURNAL OF MATERIALS SCIENCE 24 (1989) 515–522

Growth of γ-alumina on crystallographically distinct aluminium substrates

KAREL K. CZANDERNA*, KAREN J. MORRISSEY‡, CHRIS J. PALMSTRØM§, C. BARRY CARTER
Department of Materials Science and Engineering, Cornell University, Ithaca, New York 14853, USA
ROBERT P. MERRILL
School of Chemical Engineering, Cornell University, Ithaca, New York 14853, USA

The growth of γ-alumina on crystallographically distinct aluminium substrates has been studied using transmission electron microscopy and diffraction and Rutherford backscattering. Oxides grown thermally on single-crystal substrates showed a preferred epitactic orientation relationship with the substrate, while oxides grown by the same technique on polycrystalline substrates did not exhibit a preferred orientation relationship. The grain size of the oxide was found to be at least one order of magnitude smaller than the initial grain size of the polycrystalline aluminium substrate.

1. Introduction

The morphology and crystallography of aluminium oxides are dependent on both the method of preparation and the precursors from which they are formed [1]. Thus, for example, transition aluminas can be formed from a variety of oxyhydroxide and hydroxide precursors. The specific form of this precursor material has been found to be particularly important for the synthesis of high-surface-area catalytically active aluminas [2]. Transition aluminas can also be grown as thin, planar layers on top of aluminium substrates [2].

The principal uses of γ-alumina are as an adsorbent and as a catalyst, co-catalyst or catalyst support. However, little is understood about either the electronic structure of this material or its crystallography. The material is usually formed by dehydroxylating boehmite which is a crystalline oxyhydroxide; this preparation procedure is known to result in defect acid sites which are believed to be the source of the unique surface chemistry found in γ-alumina [2, 3]. Although the crystal structure of γ-alumina is thought to be that of a distorted "defect" spinel, the detailed atomic arrangement is not yet known [4, 5]. When grown on an aluminium substrate, the resulting γ-alumina provides a uniform planar sample that can be used as a model material for studying catalytically active surfaces using both transmission electron microscopy (TEM) and surface spectroscopic techniques which can be performed under ultra-high vacuum (UHV) conditions [2].

Understanding the specific role of the metallic substrate and its surface preparation on the morphology and orientation of the resulting γ-alumina is a prelude to the study of such model systems. In this study the effects of structure and preparation of the metal substrate on the morphology and crystallographic orientation of γ-alumina grown by air oxidation has been examined.

2. Experimental details

Aluminium substrates were chosen to span a variety of cold-rolling conditions and purities. Table I summarizes the types of aluminium studies together with their approximate grain size, the approximate grain size of the oxide, the preparation techniques, and the oxidation conditions. The single crystals were grown by the strain–anneal technique [6] using 6N pure aluminium (5×10^{-5} at % impurities). They were then spark-cut to the required orientation, and chemically polished. The polycrystalline coupons studied were 4N or 5N pure aluminium (5×10^{-3} or 5×10^{-4} at % impurities) that had been cold-rolled to a thickness of approximately 3 mm. The third material, Alcoa 1199-0, is used industrially as capacitor foil; it is 4N material and is specially cold-rolled to yield 80% of the surface in the $\{1\,0\,0\}$ orientation. The fourth material was Alcoa thick sheet (4N) which had been cold-rolled in the usual manner to a thickness of 2 mm. Alcoa sheet stock (4N) was also used as polycrystalline aluminium and had been cold-rolled to a thickness of 100 μm.

The single-crystal samples and one 5N polycrystalline coupon sample were mechanically polished to a mirror finish. A 4N and a 5N pure polycrystalline coupon sample were recrystallized in air at 598 K for 15 min. All of the substrates were ultrasonically cleaned using trichloroethylene (a degreaser),

* *Present address*: Eastman Kodak Company, 1669 Lake Avenue, Rochester, NY 14650, USA.
‡ *Present address*: E.I. Du Pont de Nemours & Co., Experimental Station, Wilmington, Delaware, USA.
§ *Present address*: Bell Communication Research, 31 Newman Springs Road, Redbank, NJ 07701, USA.

0022–2461/89 $03.00 + .12

followed by acetone and finally ethanol. One piece of Alcoa sheet stock was subsequently electropolished in a solution of perchloric acid and acetic anhydride at 0° C.

The substrates were oxidized in air at 863 K for 3 h, except for three pieces of Alcoa thick sheet which were oxidized for 10, 30 and 60 min, respectively. γ-alumina was grown on certain substrates for Rutherford backscattering (RBS) studies by boiling the aluminium in distilled water and then dehydrating at 671 K for 1.6 min [2].

After oxidation, the oxide was chemically removed from the aluminium substrate by immersing the sample in a saturated mercuric chloride solution until gas bubbles were observed on the sample surface. The sample was moved quickly to a Petri dish containing distilled water, where the oxide separated from the substrate and floated to the surface of the water. In some cases, the oxide film was very thick and had to be gently broken apart using two pairs of sharp tweezers. Subsequently, the oxide film was picked up on a 3 mm diameter copper TEM grid, coated with carbon, and examined using a Seimens Elmiskop 102 TEM operating at 125 kV.

Two of the films were also examined using a scanning transmission electron microscope (STEM, Jeol Temscan 200CX) equipped with an energy-dispersive X-ray spectroscopy (EDS, Tracor Northern) detector; two other films were examined using RBS. No trace impurities were observed using EDS, but RBS did show the presence of mercury contamination. Some of the oxide films separated from the substrates in pieces which were too small to be usable for TEM studies, while other oxide layers were too thin to be seen during the removal from the aluminium. Thus, the oxide grain sizes for two of the aluminium substrates are not listed in Table I; oxides grown on Alcoa thick sheet for 10 and 30 min were too thin to be removed successfully from the aluminium substrate.

The grain size of the oxide film was characterized using Martin's diameter, which is often used for analysing three-dimensional particles from sections in two dimensions [7]. The diameter of each grain encountered along a straight line across the micrograph is measured where it bisects the grain area. The term "grain" is used in this paper to describe an area of single crystal which is surrounded either by a structured or an amorphous grain boundary region. The adjacent "grain" may thus be either in the same or a different orientation. Measurement of the average Martin's diameter for a particular oxide film was determined from at least 10 different grains on each of 5 micrographs. The results and standard deviation are reported in Table I.

Aluminium samples, similar to those that were oxidized, were etched to reveal the grains using a mixture of 20 cm^3 of hydrochloric acid, 10 cm^3 of nitric acid, 0.5 cm^3 of hydrofluoric acid and 30 cm^3 of distilled water. The aluminium grain size was measured using a combination of optical and scanning electron microscopy; the grains were well defined for the 5N materials, but were difficult to discern for the cold-rolled pieces of 4N aluminium due to the surface roughness. One piece of Alcoa thick sheet was also etched after oxidation to determine the change in aluminium grain size during oxidation.

For the RBS study, a General Ionex Tandetron (tandem accelerator) was used to produce a 1.1 to 3.045 MeV He^{2+} ion beam with area 1 mm^2 and a current of 20 nA. The energies of backscattered ions were analysed using a silicon surface-barrier detector coupled to a multichannel analyser. The vacuum in the analysis chamber was usually better than 10^{-4} Pa. For helium ions scattering from an oxygen nucleus, the scattering cross-section has a narrow resonance (increase) at a collision energy of 3.045 MeV [8]. This resonance was used to increase the sensitivity for oxygen at the surface. A control sample was always measured in order to calibrate the oxygen yield for the oxygen resonance experiments. Rutherford backscattering using 1.1 MeV helium ions and glancing incidence was used to enhance the step in the aluminium

TABLE I Measurements of the average (Martin's) diameter measured in the oxide film for different preparations of the aluminium metal surface (averages of 50 measurements)

Substrate	Purity	Preparation*	Aluminium grain diameter	Oxide grain diameter
{1 0 0}	6N	Mechanical	1 cm	63 ± 26 nm
{1 1 1}	6N	Mechanical	1 cm	77 ± 39 nm
{1 1 0}	6N	Mechanical	1 cm	90 ± 30 nm
Polycrystalline	5N	Mechanical	–	123 ± 57 nm
1199-0†	4N	none	470 μm‡	135 ± 58 nm
Thick sheet†	4N	Mechanical	20 μm	138 ± 62 nm
		+ 1 h at 863 K	20 μm	104 ± 56 nm
		+ 3 h at 863 K	1.8 mm	–
Sheet stock	4N	None	3 μm	142 ± 52 nm
Recrystallized	5N	15 min at 598 K	4.5 mm	145 ± 54 nm
Polycrystalline	5N	None	420 μm	158 ± 62 nm
Sheet stock	4N	Electropolished	–	173 ± 77 nm
Polycrystalline	4N	None	20 μm	RBS
Recrystallized	4N	15 min at 598 K	30 μm	RBS

*This substrate treatment is in addition to heating for 3 h at 863° C, unless an alternative heat treatment is noted. All substrates were solvent-cleaned.
†Manufactured by Alcoa.
‡Grain diameter for the grains not oriented close to the {1 0 0} pole.

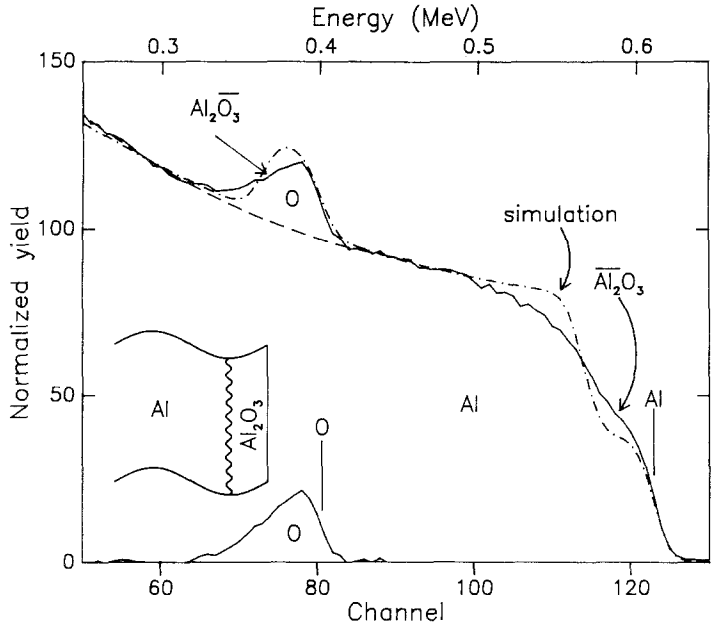

Figure 1 RBS spectrum of oxidized Alcoa thick sheet, along with a polynomial fit and background subtraction, and a simulated spectrum for Al–O on aluminium. 1.1 MeV He^{2+}, 7° tilt.

spectrum due to the formation of alumina at the surface. Analysis of this step enables the thickness of the oxide and its uniformity to be determined.

The RBS analysis was performed on a number of samples, including polished and non-polished pieces of aluminium with oxides grown in air at three temperatures: 295, 726 and 863 K, and on oxides produced by boiling in water followed by dehydration at 671 K. Most of the oxides were examined by RBS while still on the aluminium substrates, but two (oxides grown on Alcoa thick sheet and Alcoa sheet stock) were also studied after they had been chemically removed from the substrate and placed on copper TEM grids. The samples chosen for RBS were similar to those listed in Table I, and were chosen to examine how oxide thickness relates to aluminium substrate preparation and oxide growth conditions.

3. Rutherford backscattering analysis

RBS provides information on both the composition and thickness of the thin oxide films, giving the depth distribution of each component [9]. Backscattering from surface aluminium would result in a peak at energy 0.61 MeV (Channel 123 in Fig. 1) for a 1.1 MeV primary beam. Since the helium ions lose energy in traversing the target material before and after a backscattering collision beneath the surface, the width of the peak in the backscattering spectrum depends on the thickness of the layer. Fig. 1 shows experimental and simulated backscattering spectra of aluminium oxide on aluminium. In the simulated spectrum, the height of the surface aluminium peak (high-energy edge) is lower than for pure aluminium due to the formation of Al_2O_3. The rise in the spectrum at about 0.57 MeV (Channel 115) comes from scattering from the thick aluminium substrate. This moves the high background down to lower energy. The oxygen peak corresponding to oxygen in the Al_2O_3 layer is superimposed on the aluminium substrate background.

Two methods for determining the amount of Al_2O_3 were used. The first method uses a polynomial fit to the aluminium background (dashed line in Fig. 1), then subtracts the aluminium contribution leaving a peak corresponding to the scattering from oxygen. The second simulates an aluminium oxide overlayer on a metal substrate; the inflection point in the aluminium shoulder was used as a criterion for similarity between the simulation and experiment. Both of these methods have been found to give oxygen atom concentrations that are similar for the same samples. The lack of a sharp step in the experimental spectrum arises from the non-uniformities in the oxide layer. The area under the oxygen peak is proportional to the number of oxygen atoms per square centimetre. Therefore the amount of aluminium oxide can be determined using the amount of oxygen calculated from the area of this peak. The oxide thickness can be calculated by converting the number of oxygen atoms per centimetre into the total number of atoms in aluminium oxide (multiply by 5/3 for Al_2O_3), then dividing by an assumed density of aluminium oxide (atoms per cm^3).

4. Experimental results

4.1. Crystallographic analysis

Oxides grown on the mechanically polished single-crystal substrates exhibited growth patterns which were related to the crystal structure of the substrate. The diffraction patterns in Fig. 2 show that the oxide grains were rotated about the axis perpendicular to the substrate surface (e.g. note the partial rings associated with the six {2 2 0} reflections in the {1 1 1} diffraction pattern). The large number of oxide grains with similar contrast indicates that the majority of the grains were oriented epitactically with the substrate, although the average grain diameter was small (80 nm). Diffraction pattern analysis showed that, in all cases, the oxide was found to be primarily γ-alumina. None of the oxides grown on polycrystalline substrates showed a preferred orientation relationship with the substrate. Fig. 3 illustrates the grain size and shape that is typical for an oxide grown on Alcoa sheet stock, a cold-rolled 4N polycrystalline substrate. The large-area selected-area diffraction

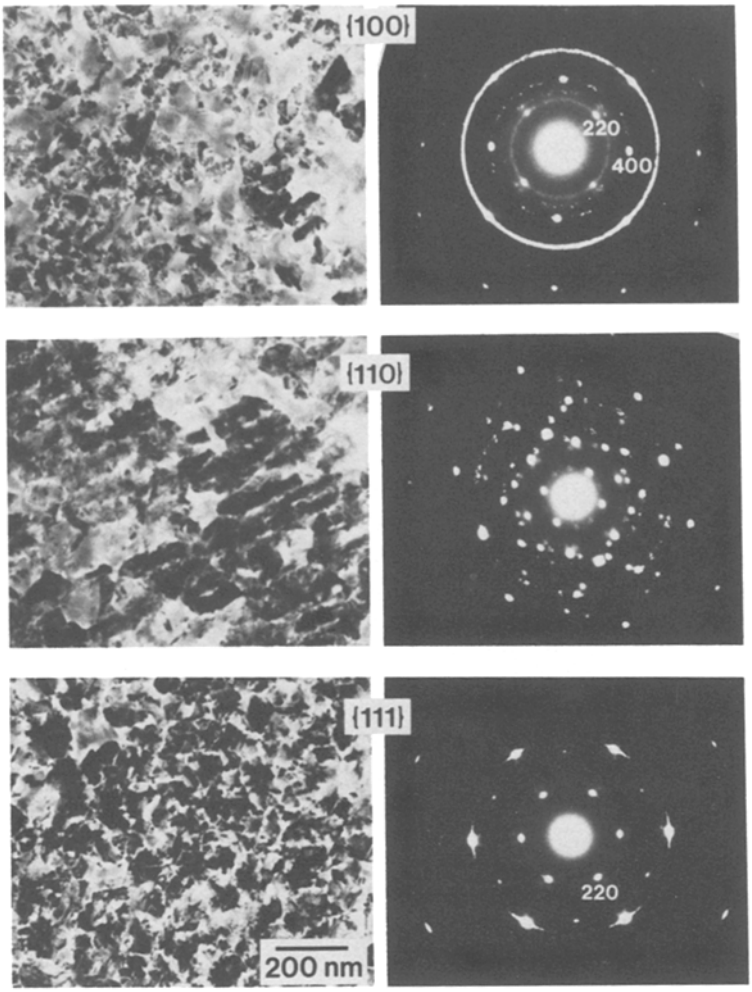

Figure 2 Bright-field images and diffraction patterns from oxides grown on Al{1 0 0}, Al{1 1 0} and Al{1 1 1}.

(SAD) pattern shows rings with few bright reflections, indicating small oxide grains with no preferred orientation. Since the single-crystal substrates were mechanically polished and most of the polycrystalline substrates were not, it was important to know whether the polishing affected the oxide growth. A piece of polycrystalline coupon was mechanically polished, and the oxide–substrate relationship was compared to that of the oxide on a non-polished piece of Alcoa sheet stock. The rings in the diffraction pattern from an oxide grown on the polished polycrystalline substrate were indistinguishable from those shown in Fig. 3b, indicating that polishing alone has very little effect on the oxide orientation with respect to the substrate.

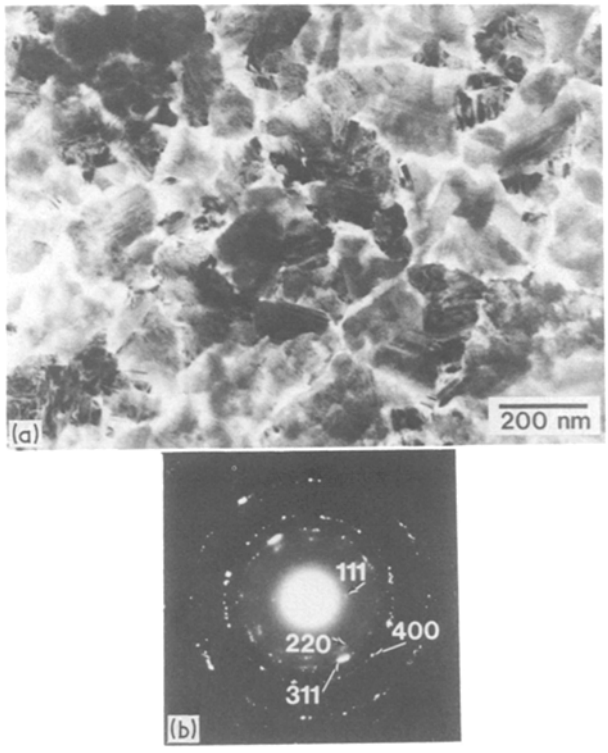

Figure 3 (a) Bright-field image and (b) diffraction pattern from an oxide grown on Alcoa sheet stock.

4.2. Grain size determination

The purity of the aluminium substrate and the degree of cold-working during rolling determines the substrate recrystallization temperature [10]. By comparing the samples before oxidation, a large difference in aluminium grain size was observed between the 5N and 4N materials. 5N material recrystallized at room temperature, whereas the 4N material did not show a substantial size change even when the material was heated at 598 K. The 5N material had a grain size similar to that seen in the 4N polycrystalline coupon directly after cold-rolling; final grain sizes are given in Table I. When this sample was heated to 598 K for 15 min, the grains became much larger (4.5 mm) than those in the corresponding 4N coupon (30 μm).

It is interesting to note the following points:

(i) Two of the 5N samples had aluminium grain sizes that were more than an order of magnitude different (4.5 mm and 420 μm), yet their oxide grain diameters were both about 150 nm.

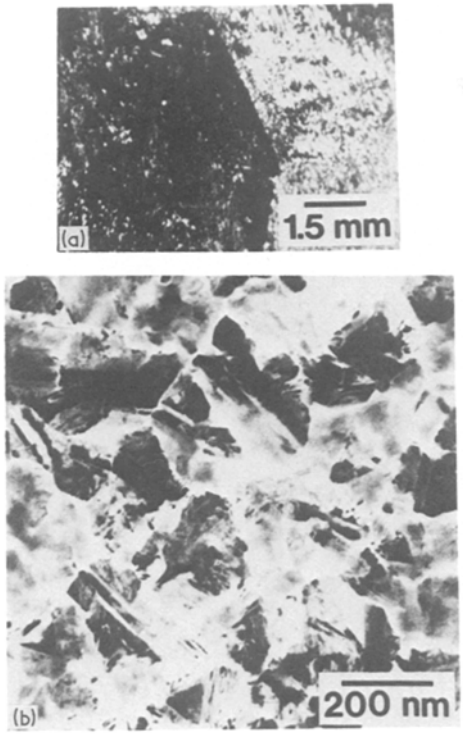

Figure 4 (a) Optical micrograph from recrystallized polycrystalline coupon and (b) TEM bright-field image of an oxide grown on a similar substrate.

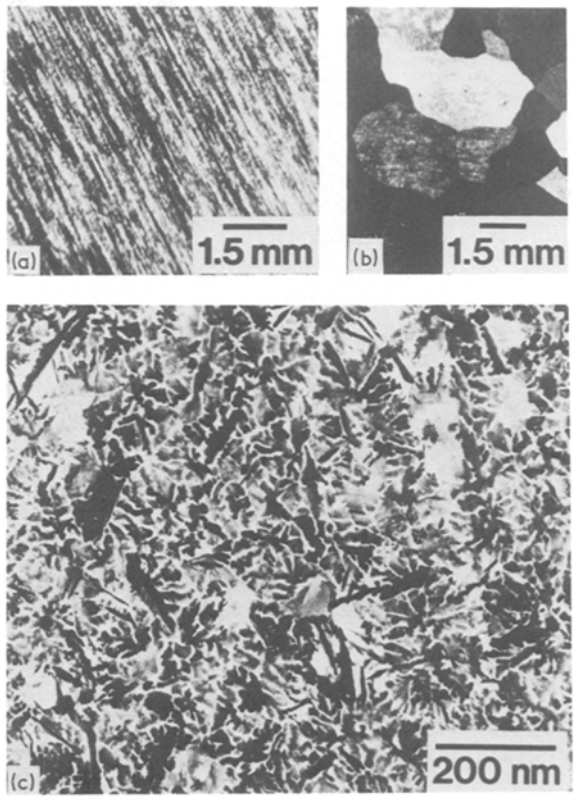

Figure 5 Optical micrographs from two Alcoa thick sheet substrates: (a) before and (b) after heating at 863 K for 3 h; (c) TEM bright-field image of the oxide.

(ii) On the Alcoa thick sheet, the grain diameter of the oxide formed by 1 h treatment at 863 K was 103 nm, i.e. smaller than the oxide diameter of 138 nm observed for the oxide formed by a 3 h heat-treatment at 863 K.

(iii) The oxide formed on an electropolished substrate had the largest observed grain diameter of 173 nm, even though the metal used had the smallest grain diameter of 3 μm before electropolishing.

The dramatic difference between the metal and oxide grain diameters is illustrated in Fig. 4: the metal (grain diameter 4.5 mm) was observed using an optical microscope while the oxide (grain diameter only 145 nm) was examined with TEM. Etched Alcoa thick sheet was also observed using an optical microscope before and after growing an oxide for 3 h at 863 K. The grain size clearly increased by several orders of magnitude during heating (compare Figs 5a and b). The oxide grain diameters for the Alcoa thick sheet and the recrystallized metal are similar (both about 140 nm, compare Figs 4b and 5c), while the grain sizes for the metal prior to recrystallization are very different (4.5 mm compared with 20 μm) as seen in Table I.

RBS was used to determine approximate oxide thickness, both as grown on the aluminium substrate and after placing films on the copper TEM grids. Table II lists the aluminium substrate the oxide was grown on, the conditions prior to and during oxide growth, the number of oxygen atoms per square centimetre, and the calculated thickness of the oxide layer in nanometres. If a density of 3.2 g cm^{-2} is assumed for all of the γ-alumina films [1], native oxides grown in air at room temperature on an electropolished single-crystal substrate were 4.8 $\pm$ 1.1 nm thick. Similar oxides on solvent-clean single-crystal and polycrystalline Alcoa sheet stock were about 8 nm thick.

Boiling aluminium in pH8, distilled water and then heating for 1.6 min at 671 K also produces γ-alumina. The thickness of this oxide was also determined for comparison with its thermally oxidized counterpart. Electropolished single-crystal and polycrystalline substrates that were boiled and then dehydrated had oxides 7 $\pm$ 2 nm thick, similar to those that were heated in air for 3 h at 726 K. Oxide grown by heating in air for one hour at 726 K was 14 nm thick. Oxides grown under identical conditions (3 h, 726 K) on solvent-cleaned substrates were baked in air at 863 K for 3 h [1], yielding oxides 80 $\pm$ 44 nm thick, with a similar oxide grown for only 1 h giving a similar thickness. The large variation in oxide thickness both as a function of substrate preparation (solvent cleaning or electropolishing) and temperature is illustrated by comparing the 100 nm thick oxide grown on solvent-clean Alcoa thick sheet for 1 h at 863 K with the 1 h, 726 K oxide grown on electropolished Al{1 1 1} that was 14 nm thick.

4.3. Oxide crystallization

Crystalline γ-alumina can be formed from an amorphous layer nucleated during air oxidation [11]. The amorphous to crystalline transition was observed by heating a particular material (Alcoa thick sheet) for different lengths of time at 863 K in air and comparing the oxide films. Fig. 6 shows amorphous aluminium oxide with some crystalline aluminium oxide nucleating with a dendritic type of grain growth. Fig. 7 shows how the dendrites grow together with another two

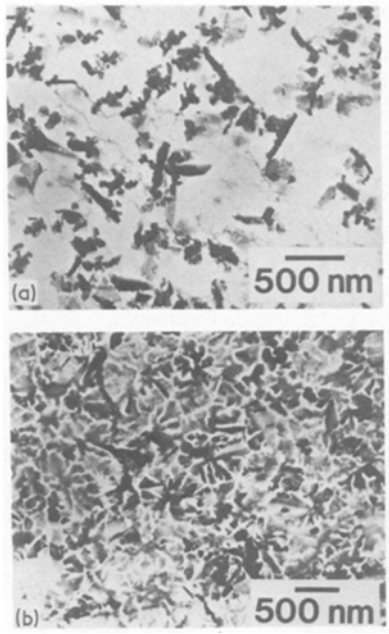

Figure 6 Oxides formed by heating Alcoa thick sheet at 863 K for (a) 1 h and (b) 3 h.

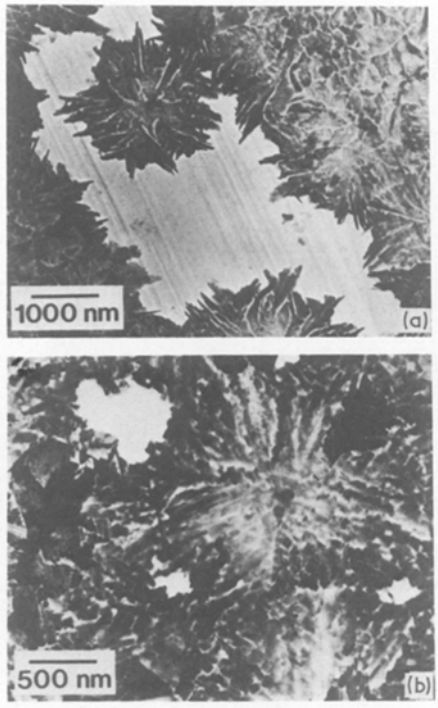

Figure 7 Dendritic grain growth: (a) polycrystalline coupon, (b) electropolished Alcoa sheet stock.

hours of heating, leaving very little amorphous alumina separating the grains. Examples of this type of growth have been given previously by Wefers [11] for surface oxides grown on aluminium alloys. The two examples shown in Fig. 7 were both observed near holes or amorphous aluminium oxide on a polycrystalline coupon, a recrystallized polycrystalline coupon, and electropolished Alcoa sheet stock even though most of the oxide was composed of densely packed grains (see Fig. 4). Note that dendritic growth was not observed on any of the oxides grown on single-crystal substrates, although the possibility of this type of growth mechanism cannot be ruled out.

Other interesting features were observed following the nucleation and growth of γ-alumina on the aluminium substrates. Fig. 8 shows an example of a series of square structures that are composed of crystalline (Area A) and amorphous areas (B and C) of oxide grown on polished polycrystalline coupon. SAD was used to determine whether an area was crystalline or amorphous and indicated that the matrix material was γ-alumina. Sometimes, such growth patterns continued for many micrometres in the oxides formed on polished Al{1 0 0} and 5N polycrystalline coupon, and on non-polished Alcoa thick sheet that was oxidized for 1 h. EDS was used to study oxides grown on both polished Al{1 0 0} and polished polycrystalline coupon to determine the composition of the amorphous areas, and the crystalline areas on the same sample. Amorphous material growing in a square pattern (Area C in Fig. 8) either surrounding, or surrounded by amorphous alumina (Area B) was also examined in the STEM using the EDS. Fig. 9 illustrates the relative amount of aluminium observed in each of the parts of this interesting growth habit by counting for the same times under the same conditions. The large aluminium peak in Fig. 9 confirms that the dark square pattern is primarily aluminium

TABLE II Summary of the thickness of the oxide films grown on different aluminium metal substrates by RBS together with the data used for the determination

Preparation conditions	Oxygen ($\times 10^{16}$ atoms per cm^2)					Oxide thickness (nm)*	
	{1 1 1}	Sheet stock	Thick sheet	Polycrystalline	Recrystallized	Average thickness	Std. error of mean
Electropolished							
As received	2.7	–	–	–	–	4.8 ± 1.1	0.4
Boiled and baked for 1.6 min at 671 K	2.7	–	–	4.5	2.4	5.9 ± 1.7	0.8
Baked for 3 h at 726 K	3.5	3.2	–	5.2	–	6.9 ± 2.0	1.1
Baked for 1 h at 726 K	8.1	–	–	–	–	14.4	–
Solvent-cleaned							
As received	4.5	1.2	–	–	–	5.0 ± 4.2	2.9
Baked for 3 h at 726 K	–	13.2	–	7.4	–	18.2 ± 7.2	5.1
Baked for 3 h at 726 K	–	–	58.8	–	–	103.9	
Baked for 3 h at 726 K	3.5	50.4	66.2	40.7	–	80.3 ± 44.2	15.6
	–	35.0	33.0	–	–		
	–	24.0†	95.0†	–	–		

*Density is assumed to be 3.2 g cm^{-3}, throughout.
†Oxide sample on copper grid.

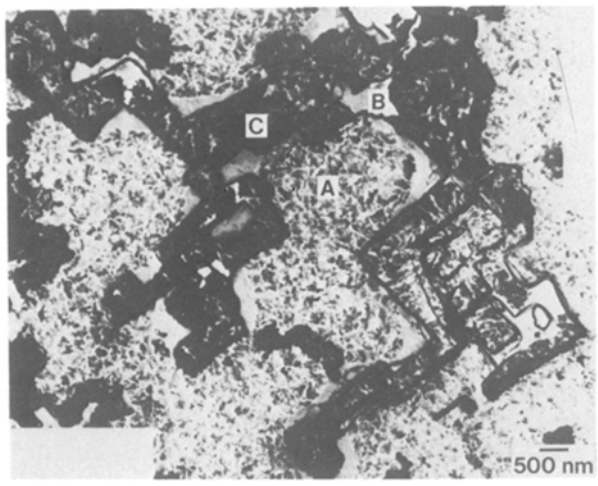

Figure 8 Growth habit observed on polished, 5N polycrystalline coupon: (A) crystalline matrix, (B) amorphous, (C) piled-up amorphous material.

oxide with small amounts of sulphur and phosphorus impurities; it usually enclosed amorphous aluminium oxide which has a much smaller aluminium signal (Fig. 9). Occasionally the amorphous aluminium oxide enclosed patches of the dark square-forming amorphous aluminium oxide to form islands of amorphous material surrounded by γ-alumina. Sulphur and phosphorus were also sometimes observed as trace impurities in both the matrix and amorphous aluminium oxide.

5. Discussion

For the ten crystallographically distinct substrates examined, γ-alumina grains were always at least one order of magnitude smaller in diameter than the grains of the respective aluminium substrate (see Table I). This implies that even on a polycrystalline substrate, the oxide nucleates on a single-crystal surface, and is not affected by the grain boundaries in the metal. In patches the size of one aluminium grain, oxide grains might be expected to be oriented with respect to the metallic substrate. In fact, little preferred orientation is actually observed on such samples. Fig. 2 illustrates this point, because all of the oxide grains shown in the bright-field image (1.2 μm across the bright-field image) should have grown on one aluminium grain (diameter 3 μm). The rings in the diffraction pattern show that the grains have a random orientation.

In the RBS spectrum for aluminium oxide on aluminium shown in Fig. 1, the aluminium edge due to aluminium oxide and the shoulder due to aluminium metal can be seen in the simulation to be very broad. This feature can be caused by the interface between the oxide and the aluminium substrate being rough as is drawn schematically at the bottom left of the figure. Samples which were cold-rolled and not polished would be expected to have a rough finish on the scale of micrometres over the ion beam width of ~ 1 mm. In contrast, the well-polished single-crystal samples had a sharper step in the aluminium spectrum as expected for the more uniform oxide layer. The large standard deviation in the number of oxygen atoms per square centimetre seen in Table II thus most likely resulted entirely from the non-uniformity of the oxide layer, which makes it difficult to determine the best approximation for the average oxide thickness.

RBS results indicated that the oxide thickness of the single-crystal specimens was within the standard deviation for all oxides (both single-crystal and polycrystalline) produced by one oxidation procedure. The factors making the largest difference in the oxide thickness were the initial aluminium surface preparation (electropolishing or solvent cleaning) and the temperature and method of growing the oxide. The oxide layers were 30 to 75% thinner on electropolished substrates than on solvent-clean metals. Native oxides were very thin (5 to 8 nm), as expected, while boiling and dehydrating, or baking

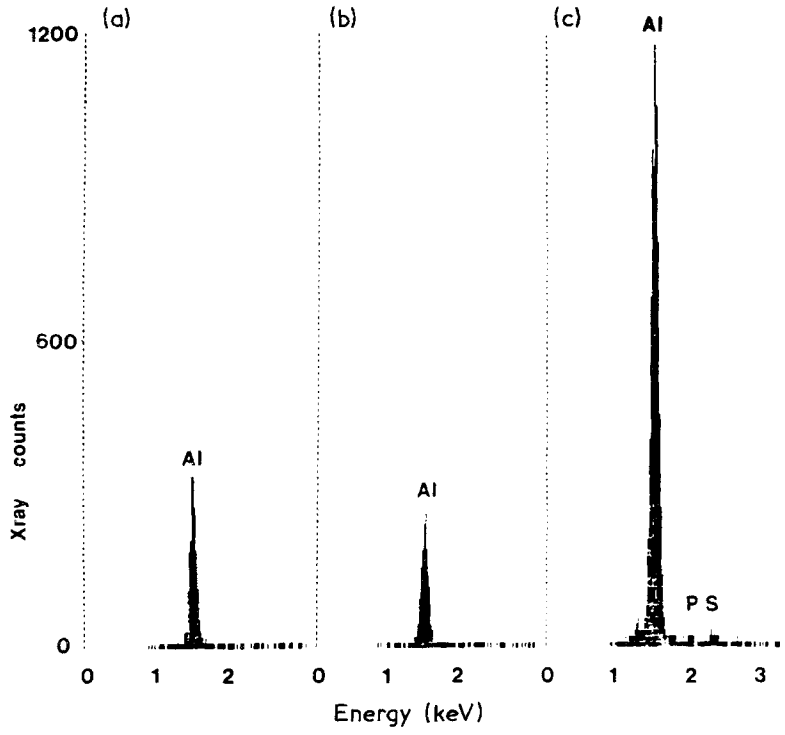

Figure 9 EDS spectra for (a) crystalline, (b) amorphous and (c) piled-up amorphous material from the oxide in Fig. 8.

at 726 K, produced oxides which were thicker (7 to 18 nm) and more suitable for TEM studies.

The formation of γ-alumina from an amorphous film was observed by studying two oxides grown under similar conditions (heating at 863 K for only 1 h or 3 h). Fig. 6 shows that γ-alumina begins nucleating in an apparently random fashion from an amorphous aluminium oxide grown on a polycrystalline substrate, starting with a dendritic type of growth and finally becoming a densely packed crystalline γ-alumina. Hart and Maurin [12] observed the nucleation and growth of oxide islands on electrolytically thinned aluminium substrates, and found the islands nucleating homogeneously throughout the amorphous oxide layer, probably at the metal–oxide interface. The dark lines seen in Fig. 6 are due to folds in the very thin amorphous alumina that probably occurred during specimen preparation. Striations in the oxide are probably due to cold-rolling marks on the aluminium substrate and were seen in the amorphous alumina from several substrates (e.g. Fig. 7). The striations may be direct evidence for a relationship between the oxide appearance and the morphology of the metal surface.

Comparing polished and non-polished 5N polycrystalline coupon in Table I shows that although polishing can decrease the oxide grain size, in this instance at least, the decrease (about 35 nm) is not large enough to explain the difference in oxide grain diameter between the single-crystal (75 nm) and polycrystalline substrates (140 nm). One explanation for the difference in oxide grain diameters is that the polycrystalline aluminium could be composed of grains oriented parallel to planes other than the low-index planes that were studied, and that these planes promote slower nucleation and/or more rapid grain growth. The role of grain boundaries in the oxide nucleation should be small, since the oxide grain size is independent of the metal grain size.

Oxides grown on polycrystalline substrates were randomly oriented, whereas on single-crystal substrates they grow epitactically. This oxide formation would not be expected if the oxide were to nucleate either within or on top of the amorphous precursor. Using Auger electron spectroscopy with depth profiling, Wefers [11] observed that on magnesium aluminium and silicon magnesium aluminium alloys, the formation of γ-alumina occurred at the metal–oxide interface. It is not clear why the epitactic growth occurs at the interface for single crystals and not for polycrystalline aluminium. Some metal oxides show a topotactic relationship on both single-crystal and polycrystalline substrates (see e.g. Ostyn and Carter [13]), but then the initial oxide formation has a crystalline character rather than the amorphous character observed for aluminium oxide. The different growth characteristics of γ-alumina compared to other metal oxides clearly requires further study.

6. Summary

Studying the growth of γ-alumina on crystallographically distinct aluminium substrates showed that single-crystal substrates yielded oxides that were highly oriented with respect to the substrate, while polycrystalline substrates produced oxides with no clear orientation relationship to the substrate. Mechanical polishing of a polycrystalline substrate decreased the grain size of the oxide slightly with respect to that of a non-polished substrate. The nucleation of the oxide is not dependent on the grain boundaries of the aluminium substrate, but begins from an amorphous precursor oxide, and occurs randomly within this amorphous layer. The aluminium oxide layer was thinner on electropolished substrates than on solvent-clean pieces of aluminium, both on unbaked and air-baked substrates. RBS showed that the grain size of the substrate material did not affect the oxide thickness.

Acknowledgements

The authors would like to thank Ms M. Fabrizio for photographic work and Professor J. W. Mayer for provision of the RBS facility. The TEM and EDS were performed in the Materials Science Center Facility for Electron Microscopy. This Facility is supported in part by NSF and maintained by Mr R. Coles. K.J.M. and C.B.C. were supported by the NSF under Grant No. DMR-8521834.

References

1. K. WEFERS and G. M. BELL, Technical Paper 19 (Aluminum Company of America, Pittsburgh, 1972).
2. D. L. COCKE, E. D. JOHNSON and R. P. MERRILL, *Catal. Rev.* **26**(2) (1984) 163.
3. B. C. LIPPENS, PhD thesis, University of Delft, Netherlands (1961).
4. K. K. CZANDERNA, K. J. MORRISSEY, R. P. MERRILL and C. B. CARTER, *J. Catal.* **89** (1984) 182.
5. S. SOLED, *ibid.* **81** (1983) 252.
6. W. G. BURGERS, in "The Art and Science of Growing Crystals", edited by J. J. Gilman, (Wiley, New York, 1963).
7. E. M. CHAMOT and C. W. MASON, "Handbook of Chemical Microscopy", Vol. 1 (Wiley, London, 1954).
8. J. R. CAMERON, *Phys. Rev.* **90** (1953) 839.
9. W.-K. CHU, J. W. MAYER and M.-A. NICOLET, "Backscattering Spectrometry" (Academic, New York 1978).
10. D. A. PORTER and K. E. EASTERLING, "Phase Transformations in Metals and Alloys" (Van Nostrand Reinhold, New York, New York, 1981).
11. K. WEFERS, *Aluminum* **57** (1981) 722.
12. R. K. HART and J. K. MAURIN, *Surf. Sci.* **20** (1969) 285.
13. K. M. OSTYN and C. B. CARTER, *ibid.* **121** (1982) 360.

Received 14 December 1987
and accepted 6 May 1988